The Astrophysical Journal, 473:L49–L53, 1996 December 10

A BURST OF HERBIG-HARO FLOWS IN NGC 1333

J. Bally[1,2] and D. Devine[2,3]
Department of Astrophysical, Planetary and Atmospheric Sciences, and Center for Astrophysics and Space Astronomy, University of Colorado, Boulder, CO 80309
and
Bo Reipurth[2,4]
European Southern Observatory, Casilla 19001, Santiago 19, Chile
Received 1996 June 7; accepted 1996 September 13

ABSTRACT

We report the discovery of over 20 groups of new Herbig-Haro (HH) objects in the NGC 1333 region of the Perseus molecular cloud, including some highly collimated jets. Our images contain over 30 groups of HH objects driven by over a dozen active outflow sources. Several of the new jets appear to be driven by optically visible stars, including HH 333, HH 334, and possibly HH 335 and HH 336. A spectacular jet, HH 333, lies nearly in the plane of the sky and has a length-to-width ratio exceeding 100 and may exhibit S-shaped point symmetry about a faint Hα emission-line star. HH 336 is located toward the cloud edge and is also centered on a visible star. A large number of new HH objects lie to the south of the concentration of known young stellar objects near SVS 13. We use published millimeter-wavelength CO and near-infrared H_2 maps and images to associate HH objects, H_2 emitting shocks, and CO outflows with more than a dozen potential driving sources. The high density of objects results in source confusion that limits the extent to which this can be done. Some HH objects are seen toward low-extinction regions far from the opaque cloud cores and may trace parts of parsec scale outflows from embedded sources. The large number of collisionally excited nebulae in this young stellar cluster requires a nearly coeval microburst of star formation.

Subject headings: stars: pre–main-sequence — stars: formation — stars: individual (NGC 1333) — infrared: ISM: lines and bands — ISM: jets and outflows

1. INTRODUCTION

Herbig-Haro (HH) objects are collisionally excited nebulae produced by supersonic outflows ejected by young stellar objects (YSOs). They trace shocks formed when faster fluid elements overtake slower ejecta (internal working surfaces) or where the outflow rams ambient cloud gas (terminal working surfaces). Since they are produced during the first few hundred thousand years of the life of a YSO, HH objects mark the approximate location of recent star formation. Outflows from YSOs may inject sufficient kinetic energy into the surrounding gas to alter the properties of the host cloud, perhaps even stopping further star formation and disrupting the cloud (Norman & Silk 1979; Bertoldi & McKee 1996), and they can be used to probe the recent mass ejection (and accretion) history of the YSO (for a recent review, see Reipurth & Cernicharo 1995).

NGC 1333 is a reflection nebula associated with a region of recent star formation in the Perseus molecular cloud for which Herbig & Jones (1983) found a distance of 350 pc and Cernis (1990) found a distance of 220 pc. A cluster of about 150 low- to intermediate-mass YSOs have been identified in near-infrared images (Aspin, Sandell, & Russell 1994; Lada, Alves, & Lada 1996). Several groups of HH objects (HH 4 through HH 18) were discovered by Herbig (1974) during the 1950s and 1960s. The group HH 7–11 was one of the first examples of a collimated jetlike outflow ejected by a young star (SVS 13; Strom, Vrba, & Strom 1976). Many far-infrared YSOs (Jennings et al. 1987), some class 0 sources (Sandell et al. 1991, 1994), a complex of overlapping CO outflows (Liseau, Sandell, & Knee 1988; Knee & Sandell 1997), and highly obscured shocks visible in the 2.122 μm H_2 line (Hodapp & Ladd 1995) are found in the NGC 1333 region. We report the detection of a large number of new HH objects in a roughly 1/4 square degree region centered near NGC 1333. We report also the discovery of several stellar jets that appear to be powered by optically visible stars.

2. OBSERVATIONS

We present wide field-of-view CCD observations of the NGC 1333 region obtained on 1995 October 23–28 with the 0.9 m f/7.5 Cassegrain telescope at Kitt Peak National Observatory with a Tektronix 2048 × 2048 CCD (T2KA), which has a scale of $0\farcs68$ pixel^{-1} and a total field of view of about $23' \times 23'$. We used narrow-band filters centered at $\lambda = 6560$ Å with $\Delta\lambda = 67$ Å for Hα observations (KP 1563), $\lambda = 6709$ Å with $\Delta\lambda = 71$ Å for [S II] observations (KP 1566), and a gunn *z* broadband filter (KP 1512), which transmits no strong emission lines excited in HH objects. HH objects can be identified by their presence in both Hα and [S II] images but absence in the gunn *z* images.

We obtained multiple 1200 s exposures through each narrow-band filter for a total exposure time of 6000 s in Hα, 6000 s in [S II] $\lambda\lambda$6717/6731, and 240 s in the far red (gunn *z*) continuum filter. Flat-fielding was based on dome flat expo-

[1] bally@casa.colorado.edu.
[2] Visiting Astronomer at Kitt Peak National Observatory, which is operated by the Association of Universities for Research in Astronomy (AURA) Inc., under contract with the National Science Foundation.
[3] devine@casa.colorado.edu.
[4] reipurth@eso.org.

TABLE 1

KNOWN NGC 1333 HH OBJECTS

Object	α (1950)	δ (1950)
HH 4B	03 26 20.34	31 09 38
HH 5A	03 26 13.81	31 02 59
HH 6A	03 26 05.94	31 08 10
HH 7	03 26 02.90	31 05 11
HH 8	03 26 00.92	31 05 17
HH 9	03 26 00.95	31 05 34
HH 10	03 25 59.95	31 05 27
HH 11	03 25 59.25	31 05 34
HH 12A	03 25 53.65	31 10 14
HH 12L	03 25 52.23	31 07 35
HH 13A	03 25 41.95	30 56 51
HH 14A	03 25 44.54	30 50 53
HH 15A	03 25 53.60	30 57 46
HH 16	03 26 02.95	30 58 52
HH 17A	03 26 14.92	31 08 16
HH 18A	03 26 21.03	30 56 58

NOTE.—Units of right ascension are hours, minutes, and seconds, and units of declination are degrees, arcminutes, and arcseconds.

sures taken through each filter. Images were reduced in the standard fashion using IRAF. Coordinates of HH objects and stars were obtained with IRAF astrometry routines using the observed positions of stars selected from the Hubble Guide Star Catalog (GSC) to fit for the geometrical distortions of the image. Coordinates are accurate to within a few arcseconds over the entire field of view.

We obtained moderate-resolution ($R \approx 6{,}000$) spectra with the 4 m Mayall reflector at KPNO on 1996 January 11 using a $2'' \times 5'$ slit on the RC spectrograph with grating KPC24 operating in the second order with a 2k × 2k CCD (T2KB). This arrangement gave a pixel scale of 0.54 Å pixel^{-1} in the red near Hα, which corresponds to a velocity resolution of about 24 km s^{-1} per pixel. The scale along the slit was $0\farcs6$ per pixel. We used a quartz lamp to obtain flat fields and a HeNeAr comparison lamp for wavelength calibration. Our spectra covered the wavelength range from [O I] λ6300 to [S II] λ6731.

3. RESULTS

Figure 1 (Plate L5) shows a color representation of the Hα and [S II] images. Figures 2 and 3 (Plates L6–L8) show sum and difference images obtained from the Hα and the [S II] data for the northern and southern sections of the NGC 1333 region shown separately. The HH objects, the plausible driving sources, and the orientation of the outflow axes (see below) are marked. The northern part of the region is dominated by the NGC 1333 reflection nebula, while the bright known HH objects are seen in the middle and lower parts of the image (Strom et al. 1986; Cohen, Jones, & Hereld 1991; Strom, Strom, & Stocke 1983; Stapelfeldt et al. 1991). Table 1 lists previously recognized HH objects in the field, and Table 2 lists the new HH objects discovered in 1995 October (see also the most recent version of the Reipurth 1994 catalog).

The silhouette of the NGC 1333 cloud core can be recognized in Figure 1. Our image of NGC 1333 can be separated into four distinct domains. The top left region is dominated by the bright reflection nebula and the bright B stars that illuminate it (yellow region in Fig. 1). The upper central portion of the image (to the lower right of the NGC 1333 reflection nebula) is dominated by the bright objects HH 6, HH 7–11, and HH 12, by bright filaments of Hα emission, and

TABLE 2

NEW NGC 1333 HH OBJECTS

Object	α (1950)	δ (1950)	Comments
HH 333A	03 26 12.83	31 16 18.4	Jet north of NGC 1333
333 star	03 26 06.05	31 15 51.0	Source of HH 333
HH 333H	03 25 51.57	31 15 15.9	
HH 334A	03 25 46.03	31 12 18.9	Jet north of HH 12
HH 335A	03 26 11.95	31 12 45.0	One-sided jet in NGC 1333
HH 336A	03 26 30.10	31 09 08.2	Jet southeast of NGC 1333
336 star	03 26 34.11	31 07 27.5	Source of HH 336
HH 337A	03 25 20.63	31 15 32.6	Filament west of HH 333
HH 338A	03 25 07.26	31 09 22.2	2′ diameter complex
HH 338G	03 25 13.08	31 07 23.8	
HH 339A	03 25 25.52	31 04 24.9	Faint north-south wisp
HH 340A	03 25 39.70	30 55 18.7	Diffuse knot
HH 341A	03 25 44.82	30 59 16.1	Bright arc
HH 342	03 25 46.52	31 00 28.7	Compact knot
HH 343A	03 25 49.06	30 55 01.7	Curved chain or jet
HH 344A	03 25 56.23	31 02 57.3	Northern knot
HH 345A	03 26 09.55	31 03 07.7	End of SVS 20 flow?
HH 346A	03 26 15.97	31 05 10.3	SVS 20 flow
HH 347A	03 26 10.24	31 05 04.3	Two knots
HH 348A	03 26 19.89	31 03 17.4	Along axis of HH 7–11 jet
HH 349A	03 26 30.72	31 03 15.6	Extension of HH 348 to east
HH 350	03 25 49.64	30 54 21.7	Hα arc south of HH 343
HH 351A	03 25 13.0	30 40 09	Very large diffuse bow shock
HH 352A	03 26 13.1	30 49 46	Two faint knots 2′ apart
HH 353	03 26 32.2	31 19 56	Large, faint, diffuse

NOTE.—Units of right ascension are hours, minutes, and seconds, and units of declination are degrees, arcminutes, and arcseconds.

very red (Hα dominated) reflection nebulosity. The region between HH 7–11 in the center and HH 14 in the south is dominated by the dark silhouette of the molecular cloud with a large number of HH objects and low level diffuse Hα and [S II] emission superimposed. Much (5%–10%) of the projected surface area of the NGC 1333 cloud is covered with HH objects having complex or "amorphous" morphology. Finally, the eastern (*left*) and western (*right*) edges of the image are dominated by relatively extinction-free regions in which a rich star field can be seen in the background.

3.1. *New Herbig-Haro Jets and Highly Collimated Flows*

Located several arcminutes north of the NGC 1333 reflection nebula, HH 333 is a highly collimated jet centered on a faint red star ("star" in Fig. 4 [Pl. L9] and Table 2) that has a bright and broad Hα emission line typical of a T Tauri star. Surprisingly, the apparent central star does not exhibit a significant near-infrared excess (Lada et al. 1996). It is possible that an edge-on disk hides the star and that all the detected light is produced by a reflection nebula. The jet has a length of about 5′ (from knot A to I) and is less than 2″ wide within 1′ of the star. Toward the western end of the jet, the knots are wider and resemble partial bow shocks. The western knot, HH 333I, has a north-to-south extent of nearly 30″. The Hα and [S II] lines are blueshifted to the west and redshifted to the east of the central star. However, these Doppler shifts are very small ($<$50 km s^{-1}), making it likely that the jet lies close to the plane of the sky. HH 337 is a north-south filament at the upper right corner of the image (northwest) about 6′ due west of HH 333I. It may be powered by the HH 333 star or, more likely, by an undiscovered source.

HH 334 is located about 1′ north of HH 12 and extends diagonally on both sides of a bright Hα emission-line star located at $\alpha(1950) = 03^{\rm h}35^{\rm m}54\fs0$, $\delta(1950) = 31°11'28''$. An isolated, possibly related, HH knot lies about 1′ beyond the

TABLE 3

NGC 1333 SOURCES AND OUTFLOWS

YSO	L[a] ($L_\odot$)	HH Objects	H_2 Shocks[b]	CO Flows[c]	P.A.[d] (deg)	Comments
333 star	?	333	?	?	260	HH jet
LkHα270	?	335	?	?	350	HH jet
334 star	?	334	?	?	115 (295)	HH jet
IRAS 6[e]	28	12	HH 12(H_2)[f]	Yes[g, h]	130	N part of HH 12
IRASf[e]	?	17	?	?	?	
IRAS 7a[e]	18/2	6	HH 6(H_2)	Yes[g, h]	44	Strong CO flow
IRAS 7b[e]	18/2	?	H_2 jet	Yes[h]	335	H_2 jet?
336 star	?	336	?	?	315	HH jet
SVS 20[i]	?	345, 346	?	?	215	
SSV 13[i]	46/3	7–11	HH 7–11(H_2)	Yes[g, h]	125	Main CO flow
SSV 13b[j]	46/3	12(?)	HL 4, 5	Yes[g, h]	175	H_2 jet
H_2O(B)[k]	46/3	ASR 20, 21, 98	Yes[h]	170	H_2 jet	
IRAS 2(N-S)[e]	42/3	(341, 342, 12)	ASR 15, 16, 49, 71	Yes[g, h]	190	Large CO flow
IRAS 2(E-W)[e]	42/3	(?)	HL 1, 2	Yes[g, h]	280	E-W CO jet
IRAS 2b[e]	42/3	(?)	(?)	Yes[h]	175	Blue CO lobe
IRAS 4a[e]	21/4	347	HL 5, 6, 10, 11, ASR 57	Yes[h, l]	215	CO jet
IRAS 1[e]	14	(338, 339, 15)	?	(?)[m, n]	140(?)	Parsec-scale flow?

[a] Luminosities taken from Jennings et al. 1987. If multiple components exist, the luminosity is divided by the number of components.
[b] ASR designations for H_2 features refer to Aspin et al 1994, and HL designations refer to Hodapp & Ladd 1995.
[c] CO outflow orientations are based on the maps presented by Knee & Sandell 1997).
[d] Position angle is measured on the plane of the sky counter-clockwise (north, east, south, west) between a north-south line and the a line drawn from a source through the center of a blueshifted outflow lobe. Two numbers, with one in parentheses that equals the first number +180, indicate that it is not known which side of an outflow is blueshifted.
[e] Jennings et al. 1987.
[f] Stapelfeldt et al. 1991.
[g] Liseau et al. 1988.
[h] Knee & Sandell 1997.
[i] Strom et al. 1976.
[j] Grossman et al. 1987.
[k] Haschick et al. 1980.
[l] Blake et al. 1995.
[m] Knee et al. 1990.
[n] Phillips et al. 1988.

eastern end of this jet near a sharp rim in the NGC 1333 reflection nebula about 2′ southeast of the star. A small bow shock lies 2′ northwest of the bright star. HH 335 is located near the core of NGC 1333 and is lost in the glare produced by reflected light in the individual narrow band or summed images. It is easy to recognize in the difference image (Fig. 2*b*). The bright star at the southern end of the jet, LkHα 270, appears to be the source. A prominent cone-shaped reflection nebula opens to the north and is symmetric about the jet axis. HH 336 extends diagonally (P.A. ≈ 135°) about 30″ to either side of a faint Hα emission-line star located at the eastern end of the NGC 1333 cloud core. The 4 m spectra show a very small blueshift ($v_{\rm lsr} > -50$ km s^{-1}) toward the northwest, a very small redshift toward the southeast, and an HH spectrum superimposed on the stellar spectrum of the driving star. HH 343 lies near the southern edge of our field, about 3′ south of the midpoint between HH 13 and HH 15. It consists of a prominent string of redshifted ($v_{\rm lsr} > 25$–125 km s^{-1}) knots. We do not have a candidate driving source for this chain of HH objects.

HH 345/346 is a collimated outflow from SVS 20 (LkHα 271). A small (5″) and bright Hα bow shock, HH 346A, emerges 10″–15″ to the southwest of SVS 20. A bubble of Hα emission surrounds this inner shock but extends nearly 1′ farther from the star. Faint Hα emission can be traced 3′ to the southwest (position angle of about 215°), which ends in a bright arc with a central knot (HH 345). Faint wisps of Hα emission northeast of SVS 20 may trace a counterflow. Our long-slit spectra show that the southwestern portion of the SVS 20 flow has a large ($v_{\rm lsr} = -50$ to -200 km s^{-1}) blueshift, while the northeastern side has a redshift with a comparable amplitude. Surprisingly, the apparent driving sources of several of the collimated flows discussed above are visible in our images.

3.2. *HH Objects,* H_2 *Shocks,* CO *Outflows, and Their Sources*

Most of the other new HH objects in our images have complex (amorphous) morphologies consisting of arcs, wisps, and partial bow shapes. We use the spatial coincidence of HH objects with shock-excited H_2 emission (see Aspin et al. 1994; Hodapp & Ladd 1995) and CO outflows (Knee & Sandell 1997; Liseau, Sandell, & Knee 1988) and clues from the orientations and shapes of HH objects to make plausible associations of the various outflow tracers with each other. We use various references from the literature to tentatively associate flows with specific driving sources (see Table 3).

The best-known HH objects in the region, HH 7–11, may be powered by the source SSV 13 (IRAS 3; Jennings et al. 1987) and are associated with the highest velocity and most-studied CO outflow in NGC 1333. A second outflow emerges from the vicinity of SVS 13 in a nearly north-south direction, possibly from the source SVS 13b (Knee & Sandell 1997), a submillimeter source 15″ southwest of SVS 13 (Grossman et al. 1987). The blueshifted CO lobe extending toward the south (P.A. = 170°) contains a 2.12 μm H_2 jet (Hodapp & Ladd 1995; HL 4 and possibly 5) that ends in a V-shaped structure about 4′ to the south. The southern portion of HH 12 is filamentary and resembles a large and fragmented bow shock. Proper motions (Herbig & Jones 1983) show that some of the gas in HH 12, 5′ north of SVS 13, is driven by a source that lies to the south, possibly SVS 13b.

The H_2O maser source B (Haschick et al. 1980), coincides with a 6 cm radio source (Snell & Bally 1986) and is located about 1′ southwest of SVS 13 at the northern end of a second filament of H_2 emission (ASR 20, 21, and possibly 98; Aspin et al. 1994) and a weak CO lobe that traces a third outflow from the SVS 13 (IRAS 3) region. To the south, the H_2 filament terminates in a bow-shaped region of H_2 emission (ASR 98) that coincides with HH 344A. HH 344B lies farther to the south in this direction and is connected with HH 344A by diffuse emission.

Knee & Sandell (1997) found a north-south bipolar CO outflow (P.A. = 190°) in the vicinity of IRAS 2 whose redshifted CO lobe also points toward HH 12. The southern (blueshifted) lobe of the IRAS 2 (N-S) flow points directly at HH 342 and HH 341, which have bow shapes consistent with excitation by IRAS 2 and which are surrounded by a faint diffuse ridge of emission extending in the general direction of this IR source. IRAS 2 also drives a second highly collimated CO jet that extends east to west (Liseau, Sandell, & Knee 1988; Knee & Sandell 1997).

The northern part of HH 12 contains an elongated [S II] filament (position angle ≈ 135°) that points back towards SVS 12 (IRAS 6). Stapelfeldt et al. (1991) found a near-IR reflection nebula associated with SVS 12 and H_2 emission pointing toward the [S II] filament that indicates that this source may power the northern portion of HH 12, confirming the earlier suggestion made by Cohen & Jones (1987). SVS 12 may also power a CO outflow at position angle 135° shown by Knee & Sandell (1997). Thus, HH 12 may be a superposition of shocks powered by at least two and possibly three sources. The [S II] bright filament at its northern edge may be powered by IRAS 6, while its brightest loops may be powered by SSV 13b and possibly IRAS 2 (N-S).

To the east of HH 12, there are two YSOs near HH 6. IRAS 7 (Jennings et al. 1987) lies about 1′ southwest of HH 6 and may power a CO flow with a blueshifted lobe coinciding with HH 6. A submillimeter source 10″ farther to the southwest of IRAS 7 may drive the H_2 jet found by Aspin et al. (1994) toward the northwest. IRASf (Jennings et al. 1987), 2′ east of IRAS 7, is a point source near HH 17.

To the southeast of HH 7–11 and SVS 20, there are several faint HH complexes, HH 348 and HH 349, which appear connected by a nearly continuous bridge of diffuse emission that can be traced to near the eastern end of the image in [S II]. These HH objects are likely powered by a source embedded in the cloud south of SVS 13. IRAS 4 is located in this general direction and consists of a pair of submillimeter sources, IRAS 4a and 4b, each of which is a close binary (Knee & Sandell 1997). IRAS 4a drives a CO jet at position angle 215° (Blake et al. 1995). Knots of H_2 emission are located symmetrically about the central source in the Hodapp & Ladd (1995) images (HL 3, 6, 10, and 11, as well as ASR 57). The northern knot, HL 11, coincides with HH 347. The source IRAS 4b also lies along a line connecting HH 349 and HH 348 and has a compact outflow. However, the millimeter-wave data do not constrain the outflow orientation (Blake et al. 1995; Knee & Sandell 1997).

IRAS 1 (IRAS 03255+3103), located about 6′ southwest of SVS 13, is a highly embedded infrared source that may drive a CO outflow with a blueshifted lobe pointing toward the southeast (Phillips et al. 1988). Knee, Cameron, & Liseau (1990), however, failed to find this flow in higher signal-to-noise data. The objects HH 339 and HH 338 lie on a line running through IRAS 1 along the orientation of the CO flow detected by Phillips et al. (1988). HH 338 looks like a fragmented bow shock moving north or northwest. HH 15 is located on the opposite side of IRAS 1 with respect to HH 338. HH 341 and 342 also lie close to the axis defined by HH 15, IRAS 1, HH 339, and the centroid of HH 338, but, as discussed above, the axes of symmetry of HH 341 and 342 are oriented toward IRAS 2 and are possibly driven by that source. The axis of symmetry of HH 15 is consistent with a bow shock moving away from IRAS 1. The alignment and morphology of HH 15, HH 339, and HH 338 make it plausible that they are powered by IRAS 1.

HH 5 and HH 18, which lie to the southeast of SVS 13, appear to be connected by faint diffuse emission. Halfway between these HH objects, there is a dark cloud core in which this emission is very faint. Both HH objects look like bow shocks facing away from this cloud core, and it is possible that they are shocks moving away from an embedded source.

Finally, two other groups of HH objects, HH 351 and HH 352, were found in the bottom portion of our images south of HH 14 (see Fig. 3). We compared the Palomar Sky Survey E-plate to our CCD images and marginally detected proper motion toward the south in HH 14, indicating that it may be driven by a source in the north. HH 14 and HH 12 have similar surface brightnesses and sizes and are both low-velocity HH objects, raising the possibility that they are opposite lobes of a parsec-scale flow, possibly from IRAS 2, which lies precisely on a line connecting HH 12 to HH 14. However, IRAS 2 is much closer to HH 12 (by a factor of more than 2) than to HH 14. Furthermore, HH 14 consists of a series of filaments oriented at position angle 45° with a faint diffuse envelope of emission that might be a large and evolved bow shock moving from the southwest, where there is a large and opaque cloud. On the other side of this cloud, a large, faint, and diffuse bow, HH 351, is seen. If we discount the marginal detection of proper motion in HH 14, it and HH 351 may trace opposite lobes of an outflow from an embedded source located between them. If these interpretations are correct, then the IRAS 1 (HH 15, 339, 338) flow and the HH 14/HH 351 (or possibly HH 12/IRAS 2/HH 14) flows are examples of parsec-scale Herbig-Haro flows. Other HH objects, especially those that lie far from cloud cores or from likely energy sources, may also be parts of giant Herbig-Haro flows.

Our observations show that there are over a dozen, and possibly several dozen, active outflow sources in the NGC 1333 clouds. YSOs are believed to drive outflows for a timescale of order 10^5 yr. To explain the observed number of HH objects and outflows, stars in this region must form at a rate of at least one to three stars every 10^4 yr, which for 0.5 $M_\odot$ stars implies a star formation rate 0.5–1.5 $\times 10^{-4}$ $M_\odot$ yr^{-1}. This rate agrees with the estimate by Lada et al. (1996) to explain the formation of 100–150 YSOs in this cluster in less than 2 Myr. The current rate of outflow activity, if sustained over time, implies that most of the stars in this region may have formed in a relatively short "microburst" of star formation with a duration much less than 1 Myr in a region with a radius less than 1 pc.

NGC 1333 is one of the most active sites of star formation in the solar vicinity. Over the central one-third of the images (between the NGC 1333 reflection nebula in the north and HH 14 in the south), about 5%–10% of the cloud surface area is covered by detectable shock-excited emission. Assuming that the depth of the region influenced by shocks is l_{pc} (in units of parsecs), that the mean velocity of the fluid producing the shocks is v_{100} (in units of 100 km s^{-1}), and that the impacting fluid elements are moving randomly, the mean time between the impact of a shock on any particular cloud element is $t = 10^5 l_{pc}/f_{0.1} v_{100}$ yr, where $f_{0.1}$ is the fraction of the cloud area covered by shocks ($f_{0.1} = 10\%$). Dissociation of molecules, followed by reformation, is expected to result in a chemically unevolved composition. Some outflows appear to be breaking out of the NGC 1333 cloud core. Such outflows may be dumping the bulk of their kinetic energy into the lower density interclump medium of the Perseus cloud and may produce bubbles and cavities in the remaining molecular gas. Such bubbles and cavities are observed in ^{13}CO maps of the region.

We thank Ralph A. Sutherland for useful discussions and the referee, Charlie Lada, for valuable suggestions. This research was supported in part by NASA grant NAGW-4590 (Origins) and NASA grant NAGW-3192 (LTSA).

REFERENCES

Aspin, C., Sandell, G., & Russell, A. P. G. 1994, A&AS, 106, 165
Bertoldi, F., & McKee, C. 1996 in Proceedings of the Symposium Held in Honor of C. H. Townes' 80th Birthday, in press
Blake, G. A., Sandell, G., van Dishoeck, E. F., Groesbeck, T. D., Mundy, L. G., & Aspin, C. 1995, ApJ, 441, 689
Cernis, K. 1990, Ap&SS, 166, 315
Cohen, M., & Jones, B. F. 1987, ApJ, 321, 846
Cohen, M., Jones, B. F., & Hereld, M. 1991, ApJ, 371, 237
Grossman, E. N., et al. 1987, ApJ, 320, 356
Haschick, A. D., Moran, J. M., Rodriguez, L. F., Greenfield, P., & Garcia-Barreto, J. A. 1980, ApJ, 237, 26
Herbig, G. H. 1974, Lick Obs. Bull., 658
Herbig, G. H., & Jones, B. F. 1983, AJ, 88, 1040
Hodapp, K. W., & Ladd, E. F. 1995, ApJ, 453, 715
Jennings, R. E., Cameron, D. H. M., Cudlip, W., & Hirst, C. J. 1987, MNRAS, 226, 461
Knee, L. B. G., Cameron, M., & Liseau, R. 1990, A&A, 231, 419
Knee, L. B. G., & Sandell, G. 1997, A&A, in press
Lada, C. J., Alves, A., & Lada, E. A. 1996, AJ, 111, 1964
Liseau, R., Sandell, G., & Knee, L. B. G. 1988, A&A, 192, 153
Norman, C., & Silk, J. 1979, ApJ, 238, 158
Phillips, J. P., et al. 1988, A&A, 190, 289
Reipurth, B. 1994, A General Catalog of Herbig-Haro Objects (ftp://ftp.hq.eso.org/pub/Catalogs/Herbig-Haro)
Reipurth, B., & Cernicharo, J. 1995, Rev. Mexicana Astron. Astrofis. (Serie de Conferencias), 1, 43
Sandell, G., Aspin, C., Duncan, W. D., Russell, A. P. G., & Robson, E. I. 1991, ApJ, 376, L17
Sandell, G., Knee, L. B. G., Aspin, C., Robson, I. E., & Russell, A. P. G. 1994, A&A, 285, L1
Snell, R. L., & Bally, J. 1986, ApJ, 303, 683
Stapelfeldt, K. R., Beichman, C. A., Hester, J. J., Scoville, N. Z., & Gautier, T. N. 1991, ApJ, 371, 226
Strom, K. M., Strom, S. E., & Stocke, J. 1983, ApJ, 271, L23
Strom, K. M., Strom, S. E., Wolff, S. C., Morgan, J., & Wenz, M. 1986, ApJS, 62, 39
Strom, K. M., Vrba, F. J., & Strom, S. E. 1976, AJ, 81, 314

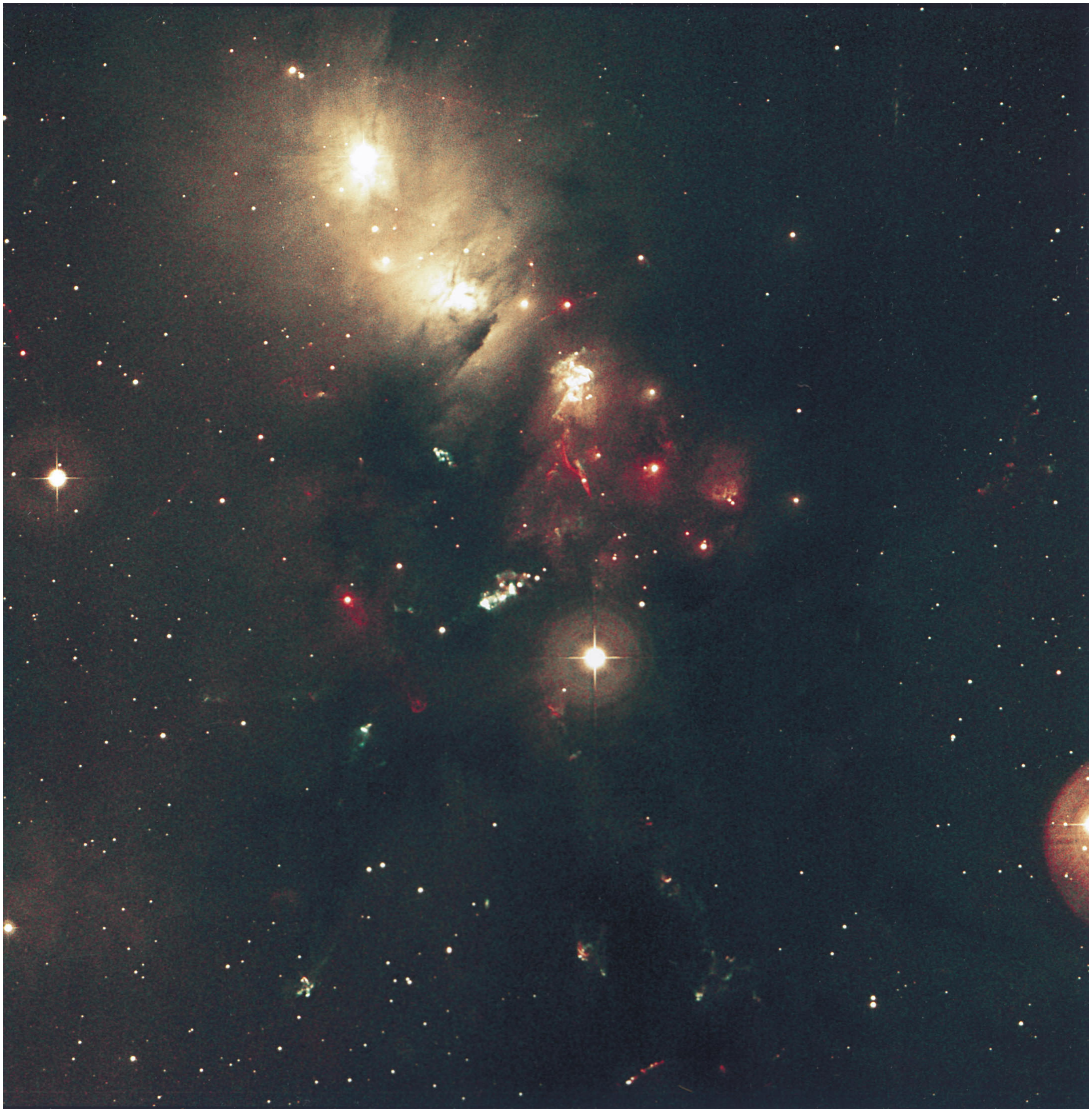

FIG. 1.—A color CCD image of the NGC 1333 region centered on SVS 13 showing Hα emission in red and [S II] in blue-green. The field of view is 23′. Total exposure time is 6000 s in each filter. North is up, and east is left.

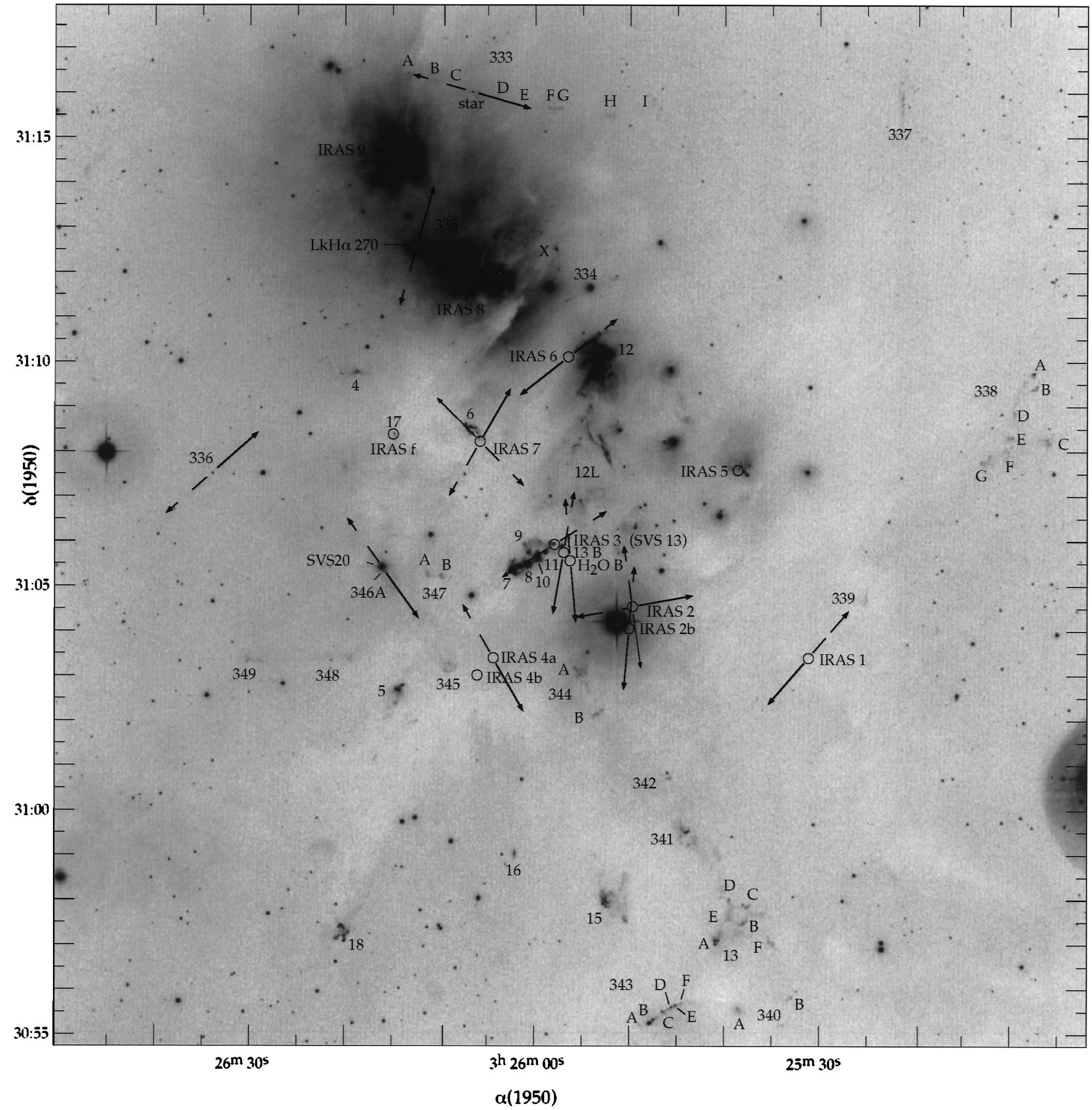

FIG. 2*a*

FIG. 2.—The northern half of the NGC 1333 field showing sum and difference images constructed from the combined 6,000 second Hα and [S II] exposures. (*a*) The sum of the Hα and [S II] images. North is up, and east is to the left. Individual HH objects and HH object clusters are labeled. Arrows show the orientations of outflows, with solid lines representing the blueshifted lobes and dashed lines representing the redshifted lobes. In the core region, the flow orientations and Doppler shifts were determined with the help of the CO data presented by Knee & Sandell (1997). For HH 333, 335, 336, and 346, the Doppler shifts and flow orientations were determined from our 4 m spectra. (*b*) The difference between the Hα and [S II] images with Hα-dominated emission in black and [S II] dominated emission in white. North is up, and east is to the left.

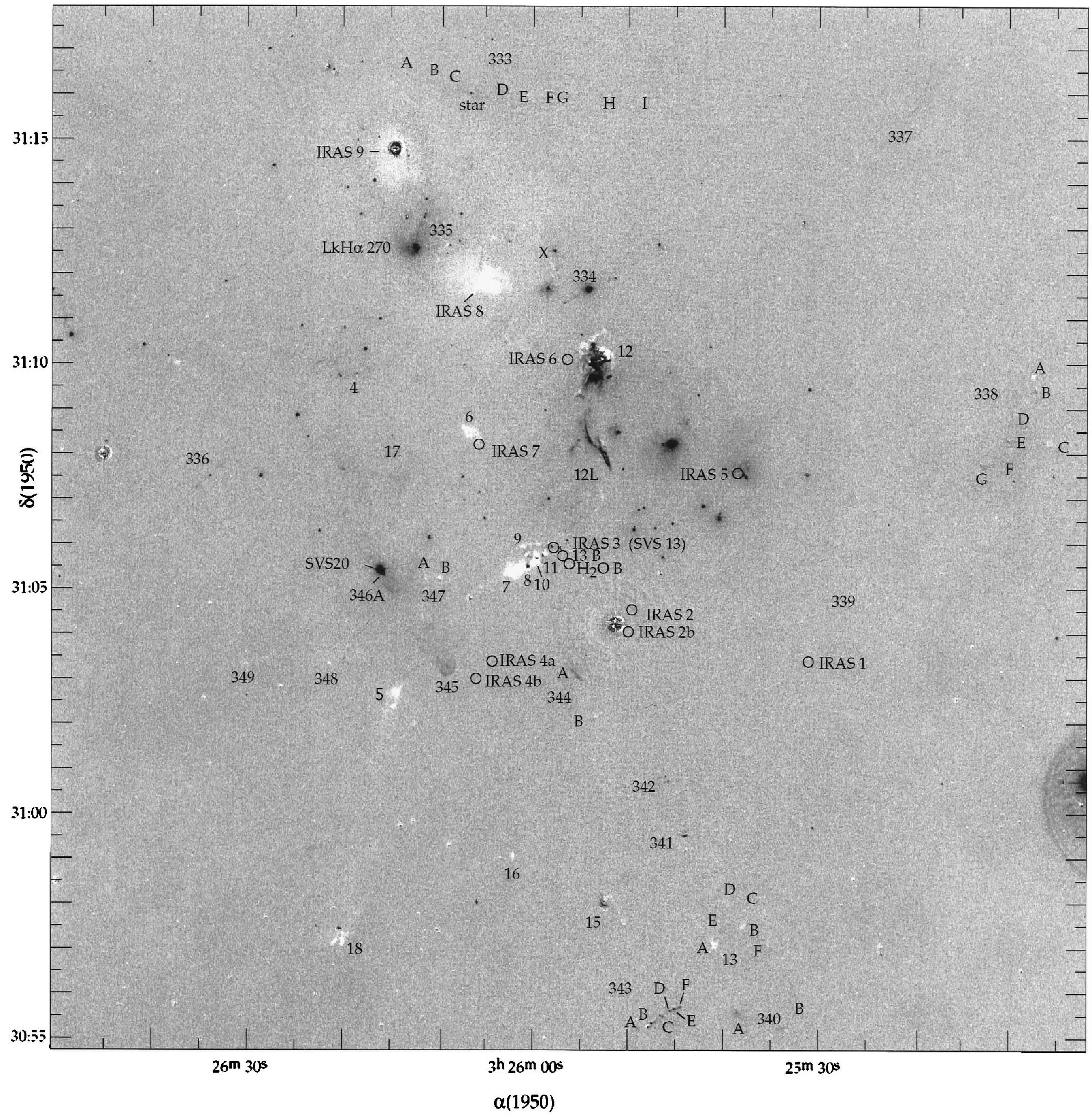

FIG. 2*b*

BALLY, DEVINE, & REIPURTH (see 473, L50)

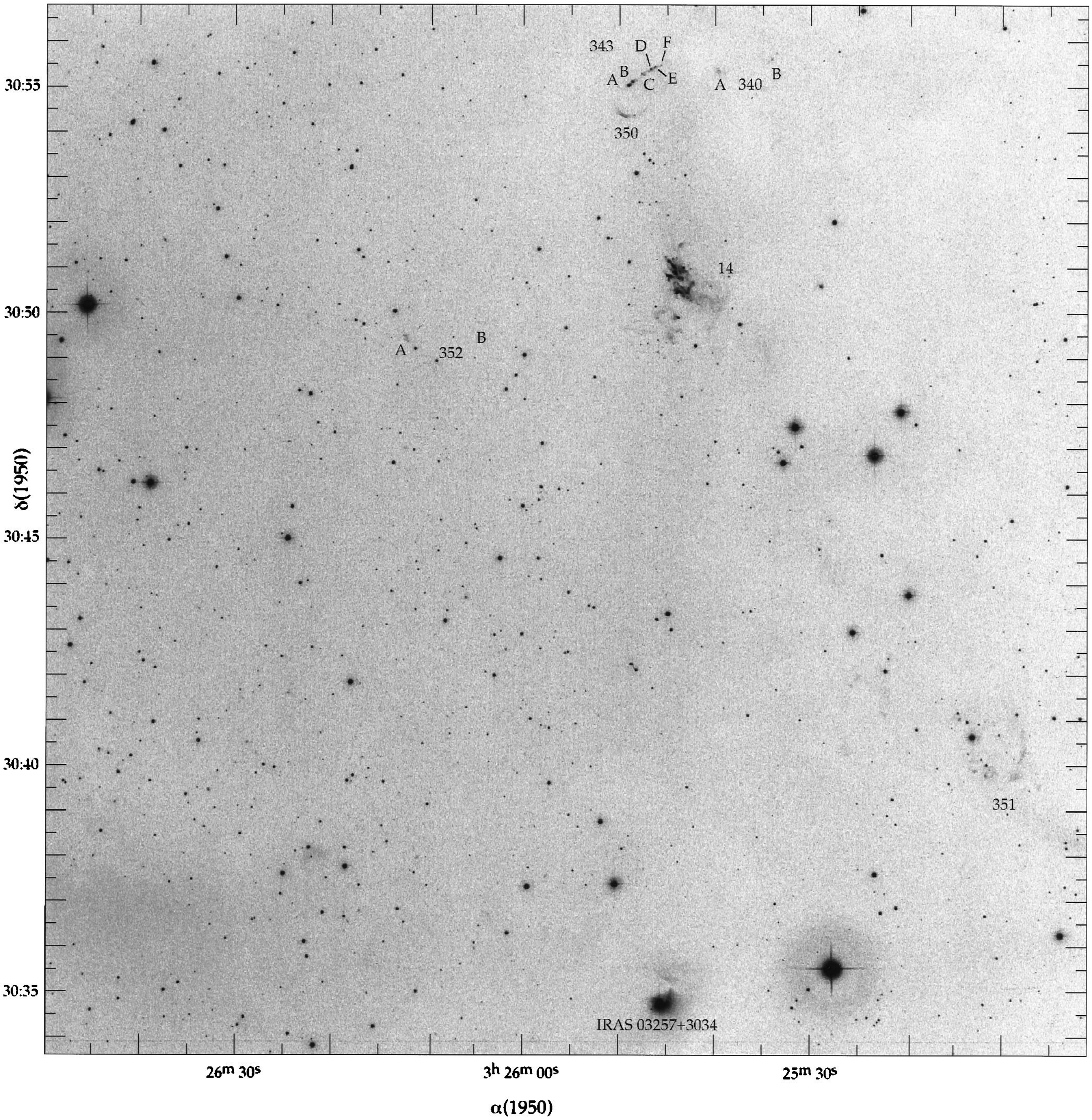

FIG. 3.—The field lying south of NGC 1333 showing the sum of Hα and [S II] images. This field contains HH 14, HH 350, HH 351, and HH 352. The difference image for this portion of the field is nearly featureless and is therefore not shown.

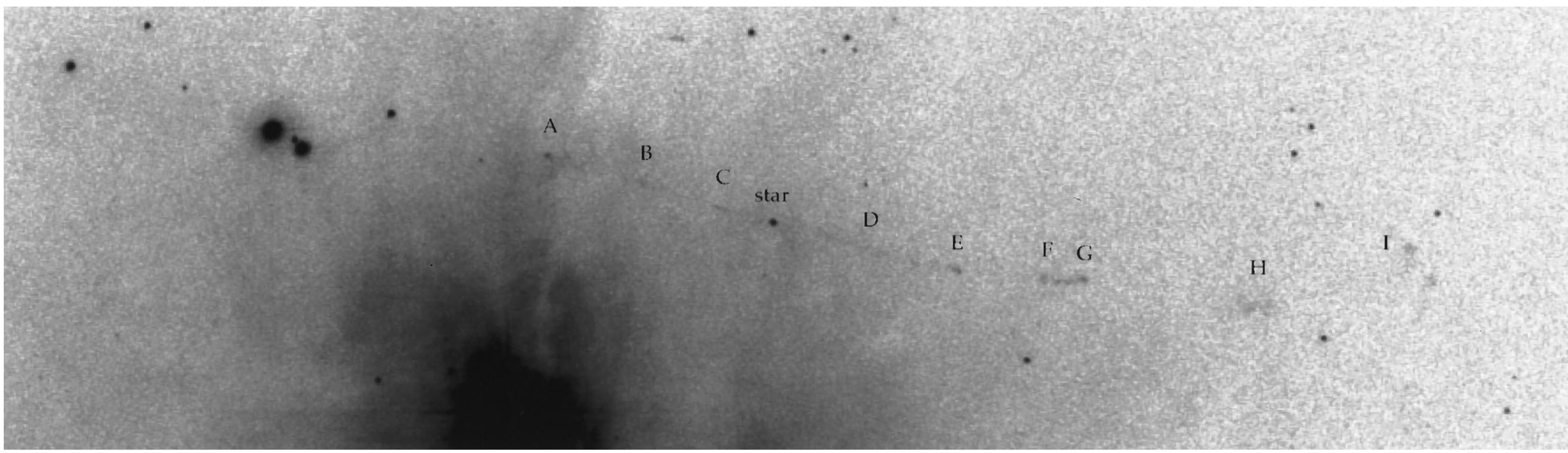

FIG. 4.—A close-up showing the HH 333 jet in Hα plus [S II]. North is up, and east is to the left.

BALLY, DEVINE, & REIPURTH (see 473, L50)